

# Toward An Assessment of Runoff and Thermal Connectivity in A River-Lake System within An Urban Environment

Y. L. Liu<sup>1</sup>, J. Z. Du<sup>1</sup>, Q. Wang<sup>1,2</sup>, W. Yang<sup>1</sup>, and B. S. Cui<sup>1\*</sup>

<sup>1</sup> State Key Laboratory of Water Environment Simulation, School of Environment, Beijing Normal University, 100875, Beijing, China

<sup>2</sup> Research and Development Center for Watershed Environmental Eco-Engineering, Beijing Normal University at Zhuhai, Guangdong 519087, China

Received 02 September 2021; revised 20 December 2021; accepted 23 December 2021; published online 30 September 2022

**ABSTRACT.** The term ‘hydrological connectivity’ is used in different disciplines to refer to the water-mediated transfer of matter, energy, and/or organisms within or between elements of the hydrologic cycle. Extensive research has been devoted to methods of evaluating hydrological connectivity. However, most of these methods pertain to the connectivity of runoff, sediment, chemicals, and organisms. To our knowledge, no evaluation of thermal energy connectivity has been conducted to date, and there is no consistent assessment framework available that takes into account thermal energy connectivity based on flux. Thermal energy flux affects many basic biogeochemical reaction processes and ecological functions of healthy river-lake systems. Here, we propose a method to evaluate runoff and thermal connectivity based on a modified version of the index of runoff/sediment connectivity proposed by Borselli et al. (2008). It was tested in an urban area (Tongling, China, which covers an area of 3008 km<sup>2</sup>) — characterized by the presence of numerous rivers and lakes — during normal, wet, and dry periods from year 2016 to year 2018. We found that areas with poor runoff connectivity exhibited high thermal connectivity in dry periods. Connectivity variation in lakes was higher than that in rivers. Models of the measured data were satisfactory for the test periods. Overall, our results indicate that public data can be used to map runoff and thermal connectivity within an existing joint evaluation framework. Evaluations of thermal connectivity can assist research on hydrological connectivity, and the proposed method can serve as a valuable tool for analyzing the runoff and thermal connectivity of urban river-lake systems.

**Keywords:** hydrological connectivity, runoff flux, thermal flux, river-lake system, spatial pattern, urbanization, impervious area

## 1. Introduction

Urban river-lake systems are different from natural ones in that they are directly related to human habitats. River-lake systems provide essential resources, such as food for urban residents, water for agriculture and farmland communities, transportation channels, and support for power generation and industrial plants (Grill et al., 2019). These rivers and lakes are located within human settlements, and as a result they are transformed, often suffering negative impacts such as significant pollution levels (Walshetal, 2005; Che et al., 2012). This highlights the nature of the existing interaction between urbanized areas and the natural environment (Binti Md et al., 2011). Urban expansion usually leads to an increase in impervious surface areas, which in turn increases runoff in urban watersheds and connectivity within river-lake systems (Paul and Meyer, 2001), modifies hydrological conditions — resulting in floods (Booth et al., 2014; Liang et al., 2020) — and poses potentially greater risks to the ecosystem ecology (Regier et al., 2020). In addition, the heat associated with urban rainfall-runoff has also become an important source of thermal pollution in river-lake systems.

\*Corresponding author. Tel.: +86 010-58802079, fax: +86 010-58802079. E-mail address: cuibs@bnu.edu.cn (B. Cui);

Considering the ongoing urban expansion, the rate at which rainfall-runoff thermal pollution contributes to the temperature increase of water bodies is currently increasing (Li et al., 2013). Urban river-lake systems are particularly sensitive to fluctuations in water temperature because temperature affects many basic processes and functions of healthy river-lake systems (Croghan et al., 2019; Grill et al., 2019).

Watershed urbanization introduces a variety of physical, chemical, and thermal stressors to the receiving river-lake systems, which are characterized by hydrological connectivity (Hassett et al., 2018). The hydrological connectivity is often used to describe the water-mediated transfer of matter, energy, and/or organisms between sources and their corresponding sink (Pringle, 2001; Pringle, 2003; Freeman et al., 2007). This includes direct connectivity via rivers or channels, and diffused connectivity, where surface runoff reaches the stream network through overland flow pathways (Croke et al., 2005). Hydrological connectivity also includes structural connectivity, which describes the spatial patterns of physical continuity among landscape units (Smith et al., 2010), and functional connectivity, which is associated with geomorphological, ecological, and hydrological processes, such as the transport of materials in a reaction system (Turnbull et al., 2008). Current research is increasingly focused on quantifying the characteristics of hydrological connectivity, including its magnitude, frequency, and flux

duration (Croke et al., 2013; Wegener et al., 2017; Wohl, 2017; Ali et al., 2018; Liu et al., 2020). However, these studies mainly examine the hydrological connectivity of watersheds under natural conditions, and do not consider the impact of urbanization, such as the effects of increased impervious surfaces on hydrology, landforms, and ecology. Therefore, a thorough analysis of the hydrological connectivity of river-lake systems within urbanized environments is needed.

Researchers have focused on the natural catchment scale to describe hydrological connectivity (Wohl, 2017; Liu et al., 2020). At present, assessments of hydrological connectivity mainly focus on determining the parameters related to water (Jencso et al., 2009; Bracken et al., 2013), sediment (Bracken et al., 2015), and chemicals (Ali et al., 2018). Liu et al. (2020) proposed a method that integrates these three variables into a unified framework. Moreover, various studies have assessed hydrological connectivity based on organisms (Crook et al., 2009; Chappell et al., 2019). Those focusing on water-mediated thermal energy are rarely conducted while studies of hydrological connectivity based on the analysis of sediments and chemicals are numerous (Webb et al., 2008; Chen et al., 2020; Horne and Hubbart, 2020). Thermal energy affects the temperature of urban river-lake systems and is an important physical variable influencing both biological and non-biological parameters, as well as water quality (Horne and Hubbart, 2020). During rainfall events, heat is transferred between rainfall-runoff and urban underlying surfaces. The runoff, heated by these, flows into the receiving river-lake system, causing an increase in the local water temperature, algal blooms, and consequent consumption of a large amount of dissolved oxygen in the water. Previous studies have considered the heat load of water bodies dispersed through road runoff (Van Buren et al., 2000; Haq and James, 2002) and mixed lands (Jia et al., 2001; Roa-Espinosa et al., 2003), but a sufficient amount of input data was not available for the model, and the results could not describe the spatial differences in detail (Janke et al., 2009). The method known as TPP (thermal pollution potential) evaluates the possibility of heat enrichment on a spatial scale, and is used to compare the potential of various types of land cover to convert available heat energy into runoff under a wide range of weather conditions (Martin et al., 2019). However, it is independent of inputs that vary with the scale of the event, such as rainfall, temperature and sunlight intensity, and thus the model is not a direct measurement of thermal energy (Martin et al., 2019). Moreover, this method based on the measurement of thermal energy cannot be compared with the existing methods used for the evaluation of hydrological connectivity, which consider water, sediment, and chemical connectivity. It is therefore essential to develop a method that can quantify the hydrological connectivity associated with thermal loading in river-lake systems at the urban catchment scale using the original framework based on water, sediment, and chemicals.

Tongling City (China) was used as a case study, as it is characterized by a typical river-lake system and its hydrological connectivity — based on runoff and thermal fluxes — has never been evaluated. We assume that runoff connectivity and thermal connectivity do not show the same spatial pattern

in Tongling City. Using publicly available data, a set of methods was developed to evaluate runoff and thermal connectivity. Firstly, thermal connectivity within a hydrological system was defined as the transport of water-mediated thermal fluxes from upstream to downstream, along a spatial gradient. Subsequently, a model of hydrological connectivity was developed based on thermal flux estimation, which was derived from a set of variables, including elevation, vegetation cover index, precipitation, impervious surface index, air temperature, and surface temperature. Finally, the spatial and temporal differences between runoff and thermal connectivity in the river-lake system within the urban context were analyzed. The predicted values of these two variables were compared to the measured water temperatures and discharge values at sampling sites in Shun'an River. The results of this study contribute to an improved understanding of hydrological connectivity in urban environments and provide essential information for water resource allocation policies to be adopted in urban catchment areas.

## 2. Materials and Methods

### 2.1. Study Area

Tongling City (30°45'12" ~ 31°7'56"N; 117°42'00" ~ 118°10'6"E), is located in southern Anhui Province, China (Figure 1a) along the lower reaches of the Yangtze River. It consists of one county and three districts (Zongyang County, Tongguan district, and Yi'an district and suburbs), covering a total area of 3008 km<sup>2</sup>, of which 355 km<sup>2</sup> are urban areas (Figure 1a). Its geomorphology is characterized by plain areas along the Yangtze River, with hills, terraces, low mountains, and other land formations present in the surrounding areas (Figure 1b). The section of the Yangtze River flowing through Tongling city is 142.6 km long and it receives considerable water input from various primary tributary sources, including the Shun'an River, Huanghu River, lakes Caizi, Baidang, Fengsha, and Chenyao, among others (Figure 1b). The water systems are distributed on both sides of the Yangtze River, and water resources depend on surface runoff, precipitation, and replenishment occurring in the area.

Tongling is characterized by a subtropical monsoon climate with mild temperatures and abundant rainfall. Based on data obtained from Tongling meteorological station, the average annual precipitation in this area is 1354 mm, and during the flood season (May to September) it reaches 784.2 mm, accounting for 57.9% of the total annual precipitation (Figure 2a). The annual average air temperature is 16.7 °C (Figure 2c). The average annual ground surface temperature is 17.9 ~ 18.0 °C, which is 1.4 °C higher than the average annual air temperature (Figure 2b).

Since 1980, nearly half of the land in Tongling has been used for agriculture, and the proportion of urbanized areas increased to 7.42 % in 2018 (Figure 2d). Tongling has a high incidence of flood events, which include both floods of the Yangtze River and floods caused by heavy rainfall (Tang, 2016; Wang, 2018). In addition, the high river temperature detected in Tongling in August 2013 was associated to an important fish mortality event in the Shun'an River (China Economic Times, 2013).

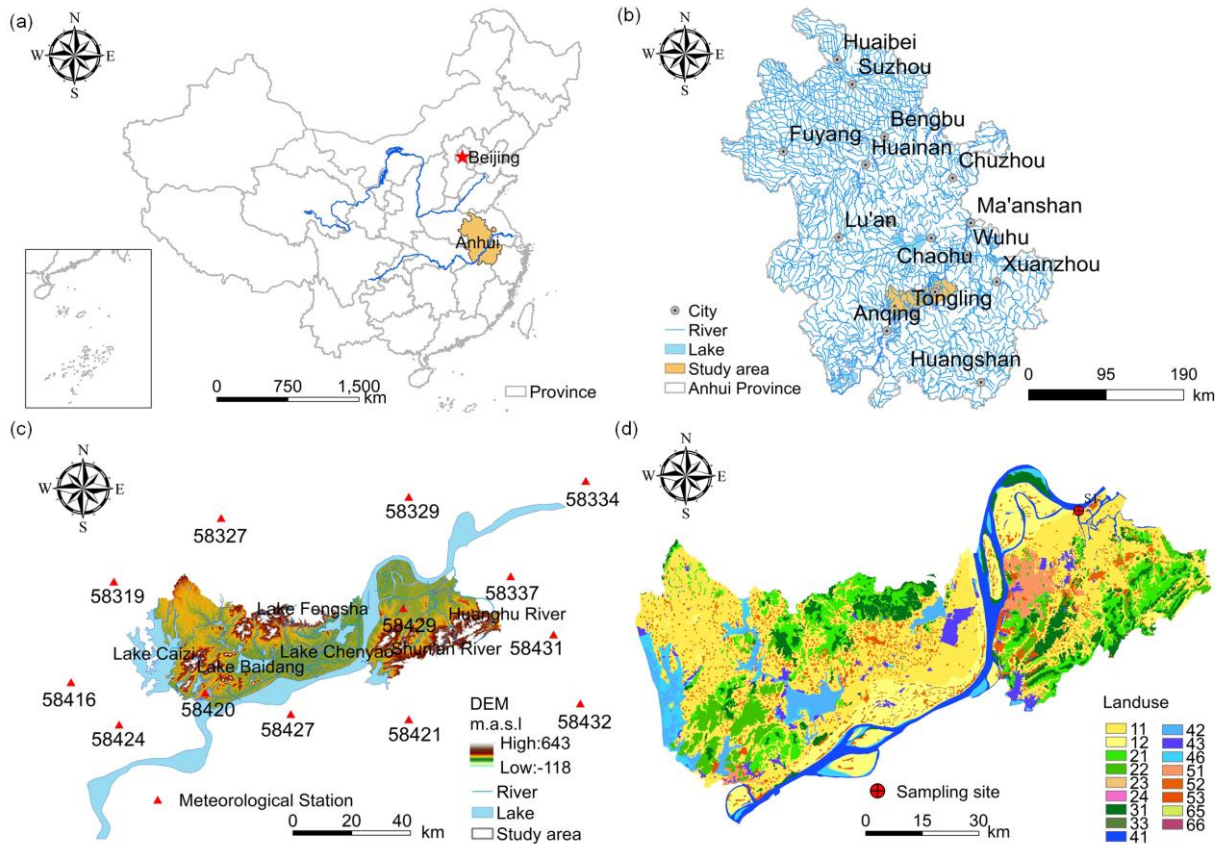


**Figure 1.** Location of Tongling City, China: (a) Location of Anhui; (b) Location of study area; (c) maps of DEM, rivers and lakes with location of meteorological stations; (d) landuse legend and sampling sites: 11, paddy field; 12, dryland; 21, woodland; 22, shrubland; 23, sparse woodland; 24, other woodlandtypes; 31, high-coverage grassland; 33, low-coverage grassland; 41, river channel; 42, lake; 43, reservoir; 46, tidal flat; 51, urban land; 52, rural settlements; 53, other construction landtypes; 65, bare land; 66, bare rock texture.

## 2.2. Definitions and Calculations

### 2.2.1. Water-Mediated Thermal Connectivity

Previous studies have provided many definitions of various aspects of hydrological connectivity, such as sediment connectivity (Bracken et al., 2015; Ali et al., 2018), chemical connectivity (Pringle, 2003; Oldham et al., 2013). Thermal energy, which is mentioned as an aspect of hydrological connectivity, has been neither clearly defined nor successfully evaluated. Therefore, in this paper a definition of thermal connectivity based on hydrological connectivity is proposed: water-mediated thermal connectivity is defined as the actual or potential thermal flux transfer that occurs during the absorption or release of heat between the elements of the hydrological cycle. It can also be understood as the water mediated-thermal flux transport from upstream to downstream, along a spatial gradient. The thermal flux associated with runoff from source A to sink B, within the catchment area, is shown in Figure 3a and is adapted from Borselli et al. (2008). The figure depicts the sources of thermal energy, its travel path and the sinks. These aspects include the initial energy carried by rainfall-runoff and which is affected by air temperature, the energy absorbed from land surfaces ( $E_g$ ,

the energy released to the atmosphere ( $E_s$ ) (but excluded from calculations), the energy absorbed from land surfaces over travel paths, and the energy output to the sink ( $E_{out}$ ). Figure 3a summarizes the parameters that affect thermal connectivity, while Figure 3b shows a theoretical watershed in grid cells, to illustrate where these thermal energy sources/paths/sinks may occur within the system (Martin et al., 2019).

### 2.2.2. Thermal Connectivity Index

Since thermal connectivity is based on runoff, the runoff connectivity in urban areas was calculated first. Kalantari et al. (2017) revised the IC index (Borselli et al. 2008) by adding a weighting factor based on surface runoff through the Soil Conservation Service (SCS) Curve Number (CN) method (SCS, 1972), which is mainly adopted in the United States. For it to be applied worldwide, this study uses the impervious surface index to calculate the runoff coefficient (Li et al., 2017). In urban areas, runoff is affected by the presence of impervious surfaces, which increase rainfall-runoff, resulting in high hydrological connectivity levels from slope to river-lake system. Therefore, the impervious surface index, precipitation, vegetation

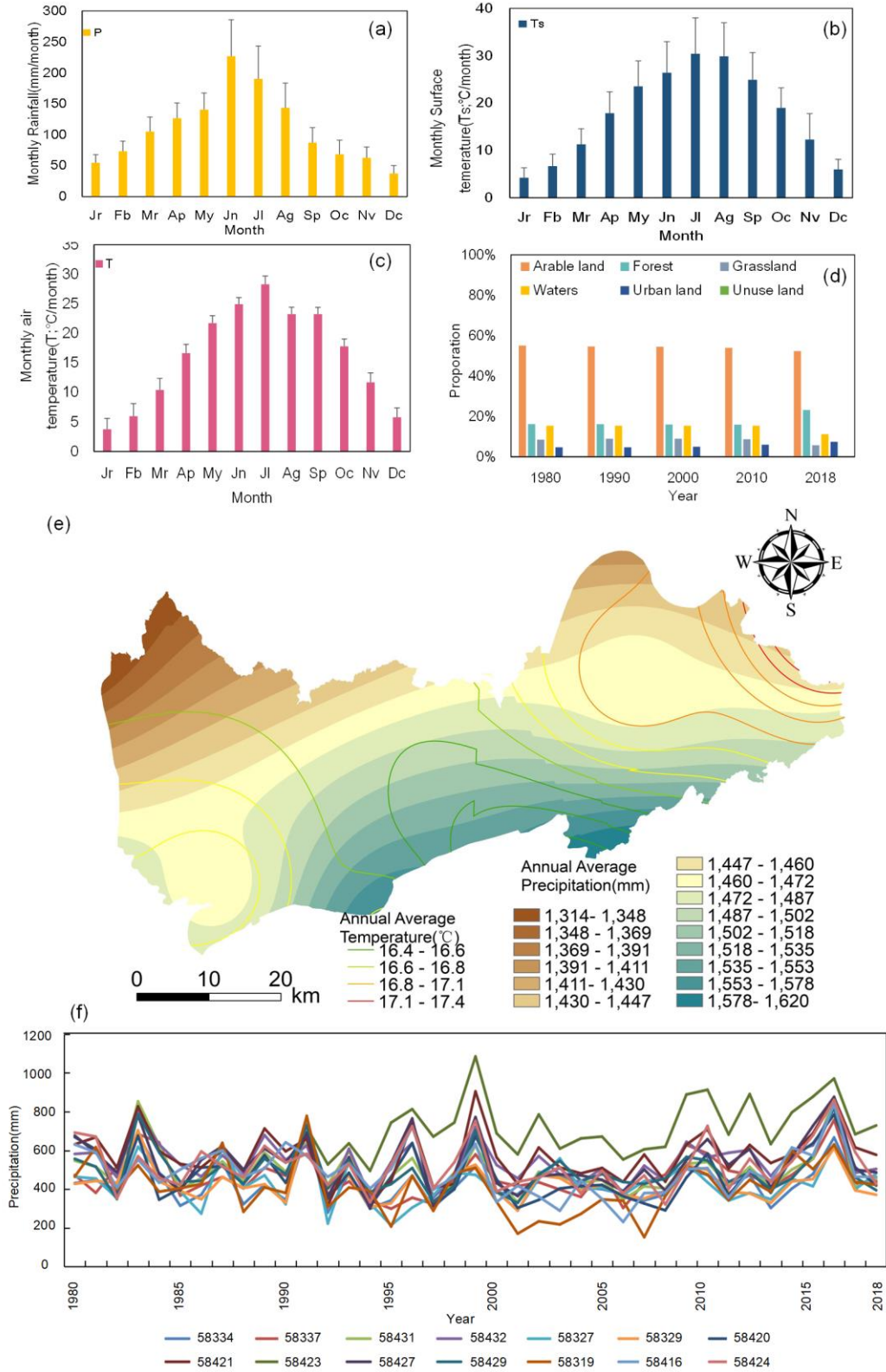


**Figure 2.** Monthly values of: (a) rainfall, (b) surface temperature, (c) air temperature, (d) statistics of land use types over a period of 40 years, (e) spatial distribution of annual average precipitation and temperature, and (f) annual precipitation from 1980 to 2018 at 14 weather stations.

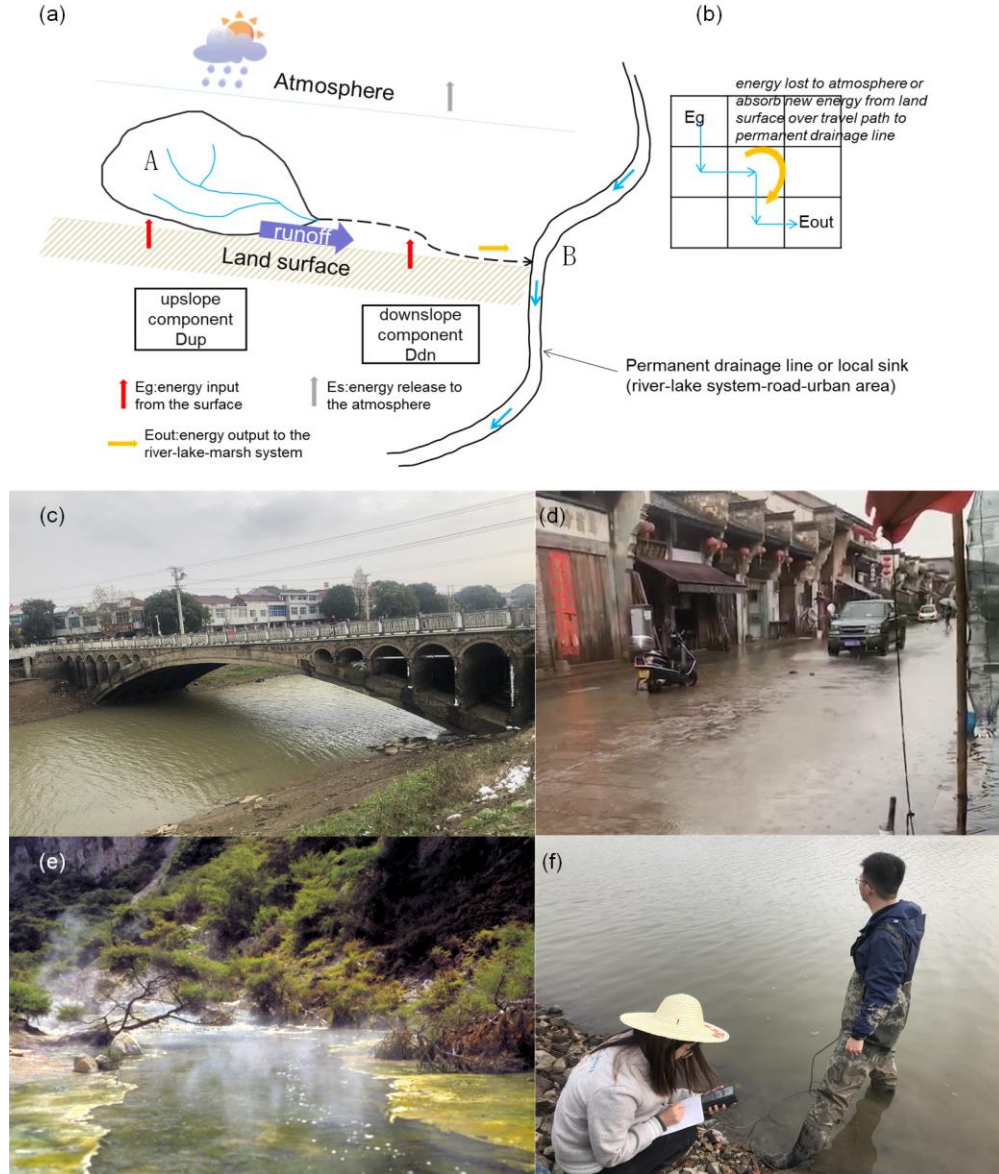


**Figure 3.** Depiction of: (a) The IC upslope and downslope component, from source A to sink B, for the runoff thermal energy connectivity index (adapted from Borselli et al., 2008); (b) A theoretical watershed with nine land cover grid cells (adapted from Martin et al., 2019); (c) Images of river, (d) impervious runoff, and (e) thermal pollution in the study area; (f) investigation photo.

coverage, land use type, and other factors are here combined with the IC, and a novel runoff connectivity assessment method, applicable to urban areas, is proposed. Based on runoff calculations used in the PLOAD model (USEPA, 2001; Endreny et al., 2003; Borah et al., 2006; Li et al., 2017), it is possible to estimate the  $IC_{runoff}$  as follows:

$$\begin{aligned}
 IC_{runoff} &= \log_{10}\left(\frac{D_{up}}{D_{dn}}\right) \\
 &= \log_{10}\left(\frac{0.01 \times \bar{P}_i \times \bar{P}_j \times \bar{D} \times \bar{C} \times \bar{S} \times \sqrt{A}}{\sum_i \frac{d_i}{AWC_{runoff}}}\right) \quad (1)
 \end{aligned}$$

$$AWC_{runoff} = 0.01 \times P_{it} \times P_j \times D_i \times C_i \times S_i \quad (2)$$

$$D_i = 0.050 + 0.009 \times I_i \quad (3)$$

where  $P$  is the rainfall (mm/a);  $P_j$  is the rainfall runoff rate (the default is 0.9) (Li et al., 2017);  $D_i$  is the surface runoff coefficient (varying between 0 and 1); and  $I_i$  is the surface impermeability index (varying between -1 and 1). The surface runoff coefficient refers to the ratio of runoff produced by rainfall, which depends on the impermeability of the underlying surface of the basin (USEPA, 2001; Endreny et al., 2003; Borah et al., 2006; Li et al., 2017). The greater the surface runoff coefficient, the more surface runoff will occur, and the greater the runoff conec-

tivity will be. Further,  $C$  represents vegetation coverage, and its value varies between 0 and 1 (Liu et al., 2020);  $A$  is the upslope contributing area ( $m^2$ );  $d_i$  is the length of the  $i$ -th cell along the downslope path (in m); and  $S_i$  is the slope gradient of the  $i$ -th cell (m/m).

The thermal energy of the surface runoff changes significantly during rainfall and is affected by the difference between rainfall temperature and surface temperature (Thompson et al., 2008; Feng et al., 2020). To calculate this thermal energy, the following assumptions are made: (i) The rainfall-runoff and the ground reach thermal equilibrium instantaneously, and temperature remains unchanged; (ii) The heat required to modify the rainfall-runoff temperature is fully derived from the surface (Feng et al., 2020). The calculation formula is:

$$Q_{runoff} = \rho \times C_p \times P_d \times \Delta T \quad (4)$$

$$\Delta T = T_s - T_r \quad (5)$$

where  $Q_{runoff}$  is the heat absorbed by rainfall from the surface;  $\rho$  is the density of rainfall, equal to  $10^3 \text{ kg/m}^3$  ( $t = 4 \text{ }^\circ\text{C}$ );  $C_p$  is the specific heat of rainfall, equal to  $4.2 \times 10^3 \text{ J/(kg}\cdot^\circ\text{C)}$ ;  $P_d$  is rainfall intensity (mm/s);  $T_s$  is surface temperature in  $^\circ\text{C}$ ;  $T_r$  is rainfall temperature in  $^\circ\text{C}$  (Xu et al., 2020); and  $\Delta T$  is the temperature variation in  $^\circ\text{C}$  caused by the transfer of heat from the ground to the rainwater runoff.

The heat and IC models were combined to propose a new method for the calculation of thermal connectivity. As shown in Figure 3, and similarly to the IC model, ‘‘Dup’’ refers to the possibility that rainfall-runoff in the upslope catchment area will absorb the available heat from impervious surfaces; ‘‘Ddn’’ refers to the potential loss or gain of runoff heat caused by the underlying surface along the line connecting the source to the sink. Due to the large scale of this study, the loss of heat due to evaporation was ignored. Therefore, the  $IC_{thermal}$  can be estimated as follows:

$$IC_{thermal} = \log_{10}\left(\frac{D_{up}}{D_{dn}}\right) = \log_{10}\left(\frac{0.01 \times \bar{P}_i \times \bar{P}_j \times \bar{D} \times \bar{C} \times \rho \times C_p \times \bar{\Delta T} \times \bar{S} \times \sqrt{A}}{\sum_i \frac{d_i}{AWC_{thermal}}}\right) \quad (6)$$

$$AWC_{thermal} = 0.01 \times P_{ti} \times P_j \times D_i \times \rho \times C_p \times C_i \times S_i \times \Delta T \quad (7)$$

### 2.3. Data Acquisition and Pre-Processing

The types of data used in this study are shown in Table 1. The flow accumulation algorithm, known as MD8, was used because it was linked to the most frequent hydrological response of the sub-catchment area and generated the most representative pattern of connectivity (López-Vicente et al., 2014; Liu et al., 2020). Terrain factors (slope and upslope contributing areas) were calculated from the DEM in ArcGIS 10.4. The index in the present study represents the potential connectivity

between hillslopes, main channels, and lakes (Cavalli et al., 2013).

In order to avoid calculation errors caused by different satellite sensing sources, all the remote sensing image data selected in this study belonged to the US Landsat series: they included image data from Landsat 4-5 TM for years 1982, 1989, 1996, and 2005, and from Landsat 8 OLI for years 2016, 2017, and 2018. Images for the year 1980 were not available, so images from 1982 were used instead. Radiometric calibration and atmospheric correction were performed on all Landsat data, based on methods described in Xu (2008). The normalized difference impervious surface index (NDISI) was calculated in ENVI, and it corresponds to  $I_i$  in the formula. The NDISI was calculated for years 1980, 1989, 1996, 2005, 2016, 2017, and 2018. Since this index shows limited variation throughout the year, for years 2016, 2017, and 2018, the NDISI of each month — belonging to each specific year — was used in the calculation of monthly connectivity. The annual normalized difference vegetation index (NDVI) values were used to generate maps of the annual C factor based on vegetation coverage (Liu et al., 2020; Wang et al., 2020). First, Landsat data were used to calculate the NDVI (Zhang et al., 2018) in ENVI5.1, and then the C factor for years 1980, 1989, 1996, 2005, 2016, 2017, and 2018 was determined. Since the vegetation in the study area did not change significantly throughout the year, for 2016, 2017, and 2018, the C factor of each specific year was used to calculate the monthly C factor.

Monthly air temperature, surface temperature, and precipitation data were obtained from 14 weather stations located within and outside the city of Tongling (Figure 1c). Monthly precipitation data from meteorological station 58416 for November 2016 and from meteorological station 58431 for August 2017 were not available; however, the amount of missing data (< 0.1%) and consequent impact on runoff analysis were considered negligible, therefore, they were not considered in the calculations. Due to the lack of surface temperature data from station 58420 for the year 1989, those for the year 1987 were used instead. As data on surface temperature, precipitation temperature, and annual precipitation were not available from station 58423 for 1989, this site was ignored for this year.

Rainfall temperature is lower than air temperature and is affected by it (Herb et al., 2008). Air temperature was used to calculate rainfall temperature, which was set as the initial runoff temperature. Measured data and back propagation (BP) calculations based on the genetic algorithm (GA) were used to predict rainfall temperature ( $T_r$ ) during the study period. Due to the lack of rainfall temperature data in the study area, rainfall and air temperature measurements obtained from Guangzhou, China, were used instead, as this area is also characterized by a subtropical monsoon climate (Feng et al., 2020). By using these substitute-datasets it was possible to establish a BP model based on GA, with a learning rate of 0.4. The monthly BP model obtained has a three-layer structure: an input layer with one variable (monthly average air temperature) is firstly linearly mapped to the intermediate variable, and then it is non-linearly mapped to the monthly average rainfall temperature of the output layer (Hsu et al., 1995). This model was used to supplement the miss-

**Table 1.** Description and Sources of the Data Used in the Connectivity Analyses

| Data                     | Description  | Source  |
|--------------------------|--|---|
| DEM                      | Raster data, 30 m resolution   | Geospatial Data Cloud URL: <a href="http://www.gscloud.cn/">http://www.gscloud.cn/</a>  |
| City boundary            | China's administrative boundary data, shp data   | Resource and Environment Data Cloud Platform<br><a href="http://www.resdc.cn/data.aspx?DATAID=201">http://www.resdc.cn/data.aspx?DATAID=201</a>                 |
| River-lake Map           | 1:1 million river polyline data, lake polygon data   | National Catalogue Service For Geographic Information<br>URL: <a href="http://www.webmap.cn/main.do?method=index">http://www.webmap.cn/main.do?method=index</a> |
| Landuse                  | Raster data, 30 m resolution in 1980, 1989, 1996, 2005, and 2014                                       | Resource and Environment Data Cloud Platform<br>URL: <a href="http://www.resdc.cn/Default.aspx">http://www.resdc.cn/Default.aspx</a>                            |
| Precipitation            | Monthly precipitation data of 14 weather stations in 1980, 1989, 1996, 2005, 2016, 2017 and 2018       | China National Meteorological Information Centre<br>URL: <a href="http://data.cma.gov.cn/data">http://data.cma.gov.cn/data</a>                                  |
| Air temperature (Ta)     | Monthly air temperature data of 14 weather stations in 1980, 1989, 1996, 2005, 2016, 2017 and 2018     | China National Meteorological Information Centre<br>URL: <a href="http://data.cma.gov.cn/data">http://data.cma.gov.cn/data</a>                                  |
| Surface temperature (Ts) | Monthly surface temperature data of 14 weather stations in 1980, 1989, 1996, 2005, 2016, 2017 and 2018 | China National Meteorological Information Centre<br>URL: <a href="http://data.cma.gov.cn/data">http://data.cma.gov.cn/data</a>                                  |
| Test data                | Monthly river water temperature data and discharge data of sampling sites in 2016, 2017 and 2018       | Environmental Protection Bureau of Tongling City, China   |

Note: DEM is the digital elevation model.

ing rainfall temperature data from Tongling city, and thus it was possible to calculate the rainfall temperature for the years 1980, 1989, 1996, 2005, 2016, 2017, and 2018 and the 36 months from 2016 to 2018. The inverse distance weighting (IDW) interpolation method was used to generate monthly and annual surface temperature maps, rainfall temperature maps and precipitation maps in ArcGIS 10.4 (Lu et al., 2008).

Calculations of connectivity indices were based on raster maps and all data were uniformed to a 30 m resolution in ArcGIS, to ensure consistency and comparability of results. All the connectivity maps were generated using the hydrology toolset in ArcGIS 10.4 (Borselli et al., 2008). The main water bodies involved in this study, lakes Caizi, Baidang, Chenyao, Fengsha, Shun'an River, and Huanghu River — which are first-level tributaries of the Yangtze River in Tongling city — were extracted to analyze the results and evaluate how the urban basin contributes to the runoff and thermal connectivity of the river-lake systems. The test data provided by the Tongling Environmental Protection Bureau, located at S1 of the Shun'an River estuary in all months from year 2016 to year 2018 (Figure 1c).

### 3. Results

#### 3.1. Spatial and Temporal Dynamics of Runoff Connectivity in Tongling City

The IC patterns of runoff connectivity from 1980 to 2016 are shown in the Appendix: Figure S1. The average values of Tongling city were -1.97, -2.01, -1.99, -2.23, and -1.57 for the years 1980, 1989, 1996, 2005, and 2016, respectively (Figure 6a). Although the mean values fluctuated, they generally showed an upward trend, which was also observed for the SD values. The trend of the IC-runoff connectivity values of most rivers and lakes was consistent with that of Tongling city, except for Lake Caizi and Lake Baidang. In addition, the SD values of Lake Caizi, Lake Liancheng, Lake Baidang, Luochang River, and Lake Fengsha increased from 1980 to 2016, while those of

Chenyao Lake, Shun'an River, Huanghu River, and Hengbu River decreased (Figure 6a).

Maps of runoff connectivity, quantified in terms of mean values for the years 2016, 2017, and 2018 were also generated on a monthly base (Appendix: Figure S3) and the trend of monthly values is shown in Figure 5. The IC-runoff showed an increasing pattern from February to July. The average values of Tongling city were -3.9302, -3.4555, and -4.7336 in April, July and December, respectively, during normal, wet, and dry periods (Figure 4). In April and December, the mean value of the Huanghu River was larger than that of the Shun'an River, while the opposite was true for the month of June. The ranking of SDs from highest to lowest among lakes and rivers did not change in any of the three months.

#### 3.2. Spatial and Temporal Dynamics of Thermal Connectivity in Tongling City

The temporal and spatial evolution of thermal connectivity from 1980 to 2016 is shown in Appendix: Figure S2. The average values of  $IC_{thermal}$  and SD showed an increasing trend from 1980 to 2016 (Figure 6b). In particular, the SD values of lakes Caizi, Liancheng, Baidang, Fengsha, and Chenyao, and both Luochang and Huanghu rivers, presented an increasing trend while they decreased for the Hengbu and Shun'an rivers.

Maps of thermal connectivity, quantified in terms of mean values for years 2016, 2017, and 2018 were also generated for months (Appendix: Figure S4). Figure 5 shows an increasing pattern for the IC value from January to July, which consequently decreases after reaching its maximum value in July. The average values of Tongling city were -2.3773, -1.6374, and -5.4769 in April, July, and December, respectively (Table 3). In July and December, the mean values of the Shun'an River were higher than those of the Huanghu River. However, the opposite was true for the month of April. The ranking of SDs from lowest to highest did not change in any of the three months. The SD value of Lake Caizi was especially high in April.

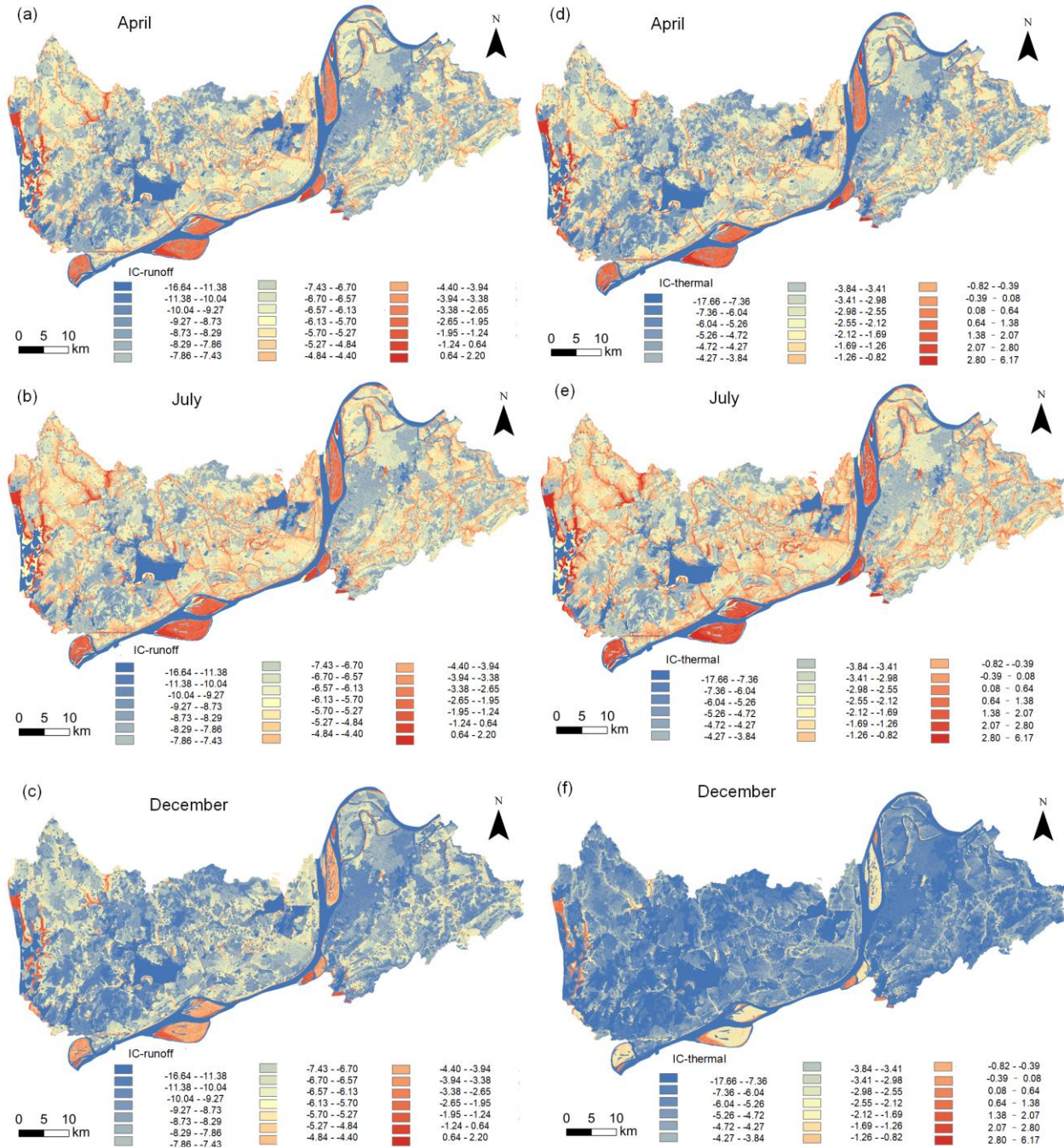


**Figure 4.** Maps of the average IC-runoff connectivity in (a) April, (b) July, and (c) December and IC-thermal connectivity in (d) April, (e) July, and (f) December.

### 3.3. Modeling Test

During the test period, the correlation between the measured data and evaluated runoff connectivity was strong ( $r = 0.793$ ): connectivity increased as water flow increased (Figure 7a). The data are evenly distributed on both sides of the trend line, with a slight deviation, indicating that runoff connectivity is closely related to traffic, but the relationship is not completely linear. The average and standard deviation of IC-runoff

connectivity and Q were plotted for each month in each sampling site (Figure 7c), revealing different temporal dynamics between IC-runoff connectivity and Q. Both variables showed an increasing trend first, followed by a decrease, and they both reached their peaks in July.

During the test period, the correlation between the measured data and evaluated thermal connectivity was strong ( $r = 0.837$ ): the water temperature increased as thermal connectivity

increased (Figure 7b). The data are evenly distributed on both sides of the trend line, with a slight deviation, indicating that thermal connectivity is closely related to water temperature, but the relationship is not completely linear. The average and standard deviation of monthly IC-thermal connectivity and T for each sampling site is shown in Figure 7d. The two variables showed similar increasing and decreasing patterns from February to August and from September to January. However, T reached its minimum in February, and IC-thermal connectivity reached its minimum in January.

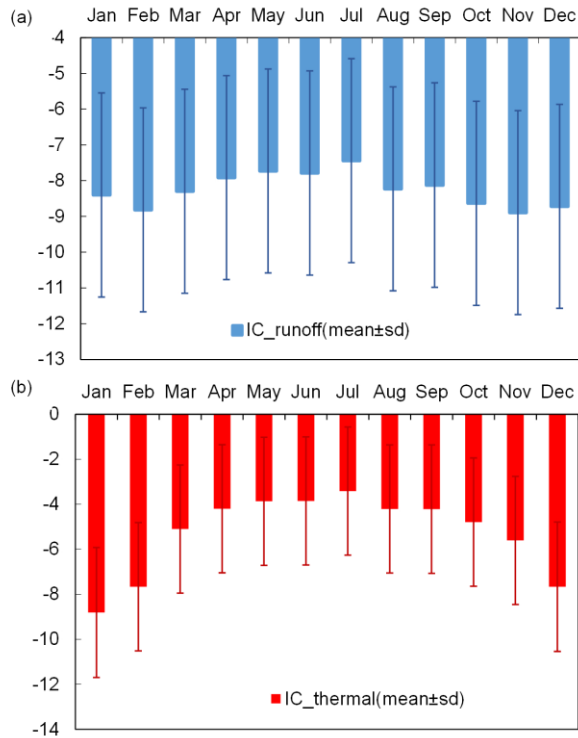


**Figure 5.** Maps of the (a) monthly temporal dynamic of the IC-runoff connectivity values in Tongling and (b) monthly temporal dynamic of the IC-thermal connectivity values in Tongling.

#### 4. Discussion

Hydrological connectivity affects the hydrological, geomorphic, and ecological functions of river-lake systems (Ali et al., 2018). However, the methods for quantifying this complex phenomenon are not currently optimal (Wainwright et al., 2011), as they fail to integrate the thermal energy aspect into the comprehensive assessment of water, sediment and chemical connectivity. We proposed a method that considers the thermal energy transported by rainfall-runoff and flowing into the receiving river-lake system. Although point sources of sewage and upstream water can affect the thermal flux, only the attribute variables related to surface thermal connectivity were considered (Covino, 2017). Despite this limitation, this method was still proven effective for the evaluation of runoff and thermal connectivity in urban watersheds.

#### 4.1. Influence of Different Variables

Although the runoff response generally varies between different regions (Vicente et al., 2014), we assumed that the surface water flow generated in the whole city was able to contribute to the river-lake system flow within the period of a single month, because its transmission distance was limited (Gomi et al., 2008). Therefore, based on these considerations, it was acceptable to use the monthly flow data for the IC model test. The estimated values of  $IC_{runoff}$  and  $IC_{thermal}$  showed a trend that was consistent with the data measured from January to December, but there were no clear outliers (high or low) in the monthly estimates compared to the measured data, especially during the wet season from May to September (Figure 7c). The difference between estimated values and measured data can be attributed to the methods employed in the analysis, which ignored the impact of the upstream section of the Yangtze River and groundwater on  $IC_{runoff}$  and  $IC_{thermal}$  (Covino, 2017). Watersheds often have a relatively large impact on the runoff and thermal connectivity of small and medium-sized rivers and lakes, while large-scale rivers are mostly affected by upstream water sources and river productivity (Webster, 2007). The interaction of precipitation and the spatial attributes of topography — i.e., vegetation coverage, land use, impervious surface, precipitation temperature, surface temperature, and air temperature — were considered in order to calculate the runoff and thermal contribution of the basin to the river-lake system (Borselli et al., 2008; Charlin et al., 2017). Generally, the proportion of low permeability surfaces is higher in urban areas, resulting in a reduction of infiltration and in an increase in the proportion of precipitation flowing through the catchment as direct surface runoff (Walsh et al., 2012; Fletcher et al., 2013).

Although previous studies of hydrological connectivity have not included thermal energy, a large body of literature exists on the factors affecting water temperature in rivers and lakes, which are a key aspect of basin thermal connectivity. Studies have confirmed that, as water flows downstream, it is less affected by the inflow of various types of runoff or tributaries, and it is more affected by ambient air temperature (Sino-krot et al., 1993; O'Driscoll, et al., 2006). The non-uniform variation of many geographical aspects, such as riparian vegetation, geology, urbanization, slope, elevation and catchment size, have also different effects on water temperature in river-lake systems (Webb et al., 1997). River inputs from the surrounding lands may have a greater impact near upstream water sources and during low flow periods than they may have further downstream during high flood periods (Pollock et al., 2009; Petty et al., 2012). Finally, in addition to the influence of water volume and air temperature on the water temperature of rivers, complex land use is also an essential variable to be considered in the analysis.

Nelson and Palmer (2007) observed that the duration, frequency, and intensity of rainfall events affect river temperature, and they should be considered in the quantification of the impact of surface runoff on the heat of river-lake systems in the further study (Herb et al., 2008). At present, the event means temperature (EMT) is the most commonly used runoff temperature index, but it is difficult to monitor at the watershed scale

**Table 2.** Descriptive Statistics of the IC-Runoff Connectivity Values Estimated in Different Months and Rivers/Lakes

| Location       | Apr.  |      |       |      | Jul.  |      |       |      | Dec.   |       |       |      |
|----------------|-------|------|-------|------|-------|------|-------|------|--------|-------|-------|------|
|                | Min.  | Max. | Ave.  | SD   | Min.  | Max. | Ave.  | SD.  | Min.   | Max.  | Ave.  | SD   |
| Caizi Lake     | -8.69 | 1.44 | -3.95 | 3.04 | -8.05 | 2.15 | -3.29 | 3.05 | -9.95  | 0.28  | -5.18 | 3.05 |
| Liancheng Lake | -6.76 | 1.73 | -3.77 | 3.11 | -6.12 | 2.36 | -3.14 | 3.11 | -8.02  | 0.47  | -5.03 | 3.11 |
| Baidang Lake   | -9.32 | 1.65 | -5.95 | 1.91 | -8.76 | 2.24 | -5.37 | 1.91 | -10.66 | 0.33  | -7.28 | 1.91 |
| Luochang River | -9.32 | 1.75 | -2.37 | 2.74 | -8.72 | 2.39 | -1.74 | 2.76 | -10.59 | 0.55  | -3.61 | 2.76 |
| Fengsha Lake   | -8.19 | 1.69 | -5.31 | 2.50 | -7.67 | 2.20 | -4.79 | 2.50 | -9.46  | 0.47  | -6.55 | 2.50 |
| Chenyao Lake   | -9.32 | 0.92 | -4.01 | 2.87 | -8.82 | 1.40 | -3.52 | 2.87 | -10.55 | -0.33 | -5.27 | 2.86 |
| Hengbu River   | -6.68 | 1.11 | -0.79 | 0.84 | -6.19 | 1.64 | -0.26 | 0.85 | -7.98  | -0.20 | -2.11 | 0.84 |
| Shunan River   | -8.87 | 2.12 | -3.12 | 1.83 | -8.39 | 2.53 | -2.65 | 1.83 | -10.03 | 0.84  | -4.34 | 1.82 |
| Huanghu River  | -5.29 | 0.92 | -3.09 | 0.94 | -4.87 | 1.34 | -2.67 | 0.94 | -6.55  | -0.32 | -4.33 | 0.94 |

**Table 3.** Descriptive Statistics of the IC-Thermal Connectivity Values Estimated in Different Months and Rivers/Lakes

| Location       | Apr.  |      |       |      | Jul.  |      |       |      | Dec.  |      |       |      |
|----------------|-------|------|-------|------|-------|------|-------|------|-------|------|-------|------|
|                | Min.  | Max. | Ave.  | SD   | Min.  | Max. | Ave.  | SD   | Min.  | Max. | Ave.  | SD   |
| Caizi Lake     | -6.23 | 3.88 | -1.50 | 4.04 | -5.32 | 4.87 | -0.56 | 3.05 | -9.00 | 1.17 | -4.26 | 3.06 |
| Liancheng Lake | -4.30 | 4.18 | -1.32 | 3.11 | -3.39 | 5.08 | -0.41 | 3.11 | -7.06 | 1.41 | -4.07 | 3.11 |
| Baidang Lake   | -6.87 | 4.09 | -3.50 | 1.91 | -6.02 | 4.96 | -2.64 | 1.91 | -9.76 | 1.24 | -6.38 | 1.91 |
| Luochang River | -6.87 | 4.19 | 0.07  | 2.74 | -5.99 | 5.13 | 0.98  | 2.76 | -9.69 | 1.45 | -2.70 | 2.77 |
| Fengsha Lake   | -5.74 | 4.13 | -2.86 | 2.50 | -4.93 | 4.93 | -2.06 | 2.50 | -8.58 | 1.35 | -5.66 | 2.51 |
| Chenyao Lake   | -6.87 | 3.36 | -1.56 | 2.87 | -6.09 | 4.13 | -0.78 | 2.87 | -9.65 | 0.73 | -4.37 | 2.86 |
| Hengbu River   | -4.23 | 3.55 | 1.65  | 0.84 | -3.46 | 4.46 | 2.48  | 0.85 | -7.11 | 1.27 | -1.19 | 0.87 |
| Shunan River   | -6.41 | 4.60 | -0.66 | 1.84 | -5.64 | 5.37 | 0.09  | 1.84 | -9.04 | 2.09 | -3.32 | 1.88 |
| Huanghu River  | -2.85 | 3.36 | -0.65 | 0.94 | -2.14 | 4.07 | 0.06  | 0.95 | -5.74 | 0.56 | -3.52 | 0.98 |

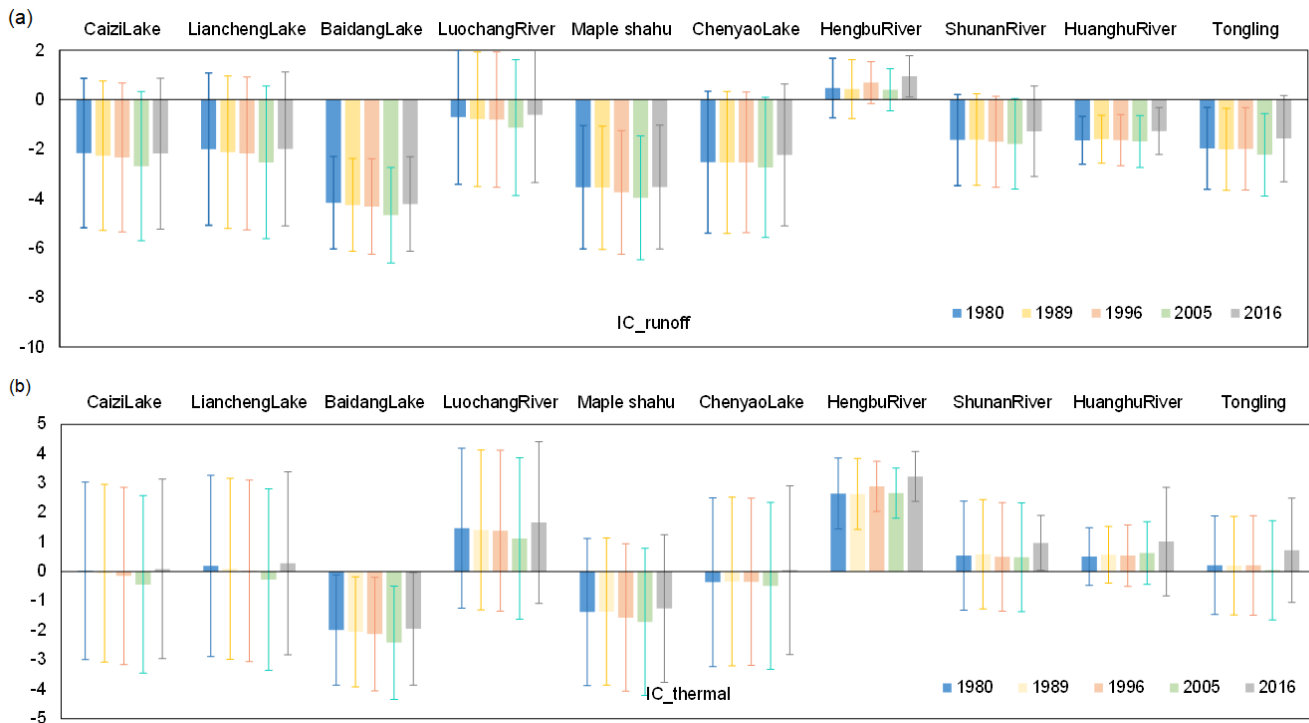


**Figure 6.** Bar plots showing (a) mean IC-runoff connectivity and (b) IC-thermal connectivity values of the rivers/lakes in 1980, 1989, 1996, 2005, and 2016. Error bars represent standard deviations.

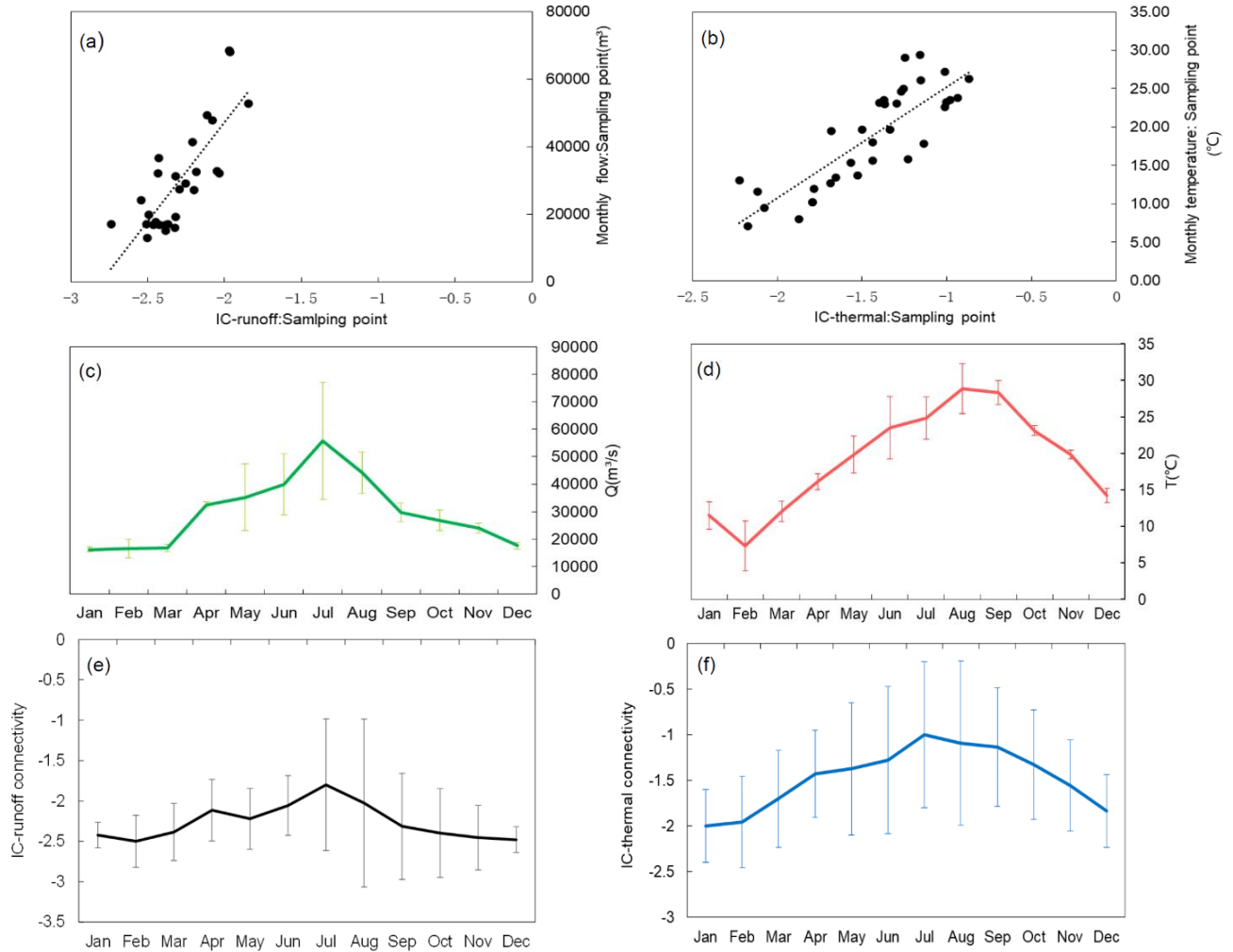


**Figure 7.** Correlation between the monthly measured values and calculation values (a) IC-runoff and (b) IC-thermal; Monthly temporal dynamics at each sampling site (c) discharge, (d) river temperature, (e) IC-runoff, and (f) IC-thermal.

(Sabouri et al., 2013). The present study, focused on the estimation of the heat impact of non-point source runoff on the river-lake systems, but ignored the heat impact of point source wastewater. Kinouchi et al. (2007) showed that a positive correlation exists between the increase in annual river temperature and the increase in the heat input derived from water treatment plants. In addition, studies have shown that the construction of reservoirs affects water temperature, and consequently the distribution ranges and breeding success of aquatic organisms (Freeman et al., 2007; Biemans et al., 2011). These aspects have not been taken into account in the present study.

The river-lake systems in this study includes the primary tributaries of the Yangtze River, which are affected by precipitation, and the water flowing from the upper reaches of the Yangtze River itself. Future investigations are needed to further evaluate the impact of this river on river-lake system. Despite the limitations previously mentioned, the proposed method can effectively evaluate the connectivity related to runoff and thermal energy at the urban watershed scale especially with small and medium-sized river-lake systems, and the results can pro-

vide relevant information to be used in environmental planning and management of urban areas.

#### 4.2. Spatial and Temporal Dynamics of Runoff and Thermal Connectivity

Lake Baidang is one of the main tributaries of the Yangtze River, and its water sources include precipitation, runoff, and the Yangtze River itself. Previously published data show the water levels of Lake Baidang during several major flood events in different years. The water levels in 1980, 1989, 1996, and 2016 were 14.08 m, 13.25 m, 14.51 m, and 15.26 m, respectively (Wang, 2018). The latter is the highest water level reached by the Yangtze River in Anhui Province (Tang, 2016), which is consistent with the evaluation results of  $IC_{runoff}$  in this study (Figure 8). However, Lake Baidang, being a “sink”, does not present high levels of connectivity, which contradicts the results obtained by Cavalli et al. (2013). The water collected from the basin and flowing into the lake is concentrated in the area around it, which presents high connectivity, due to its high slope

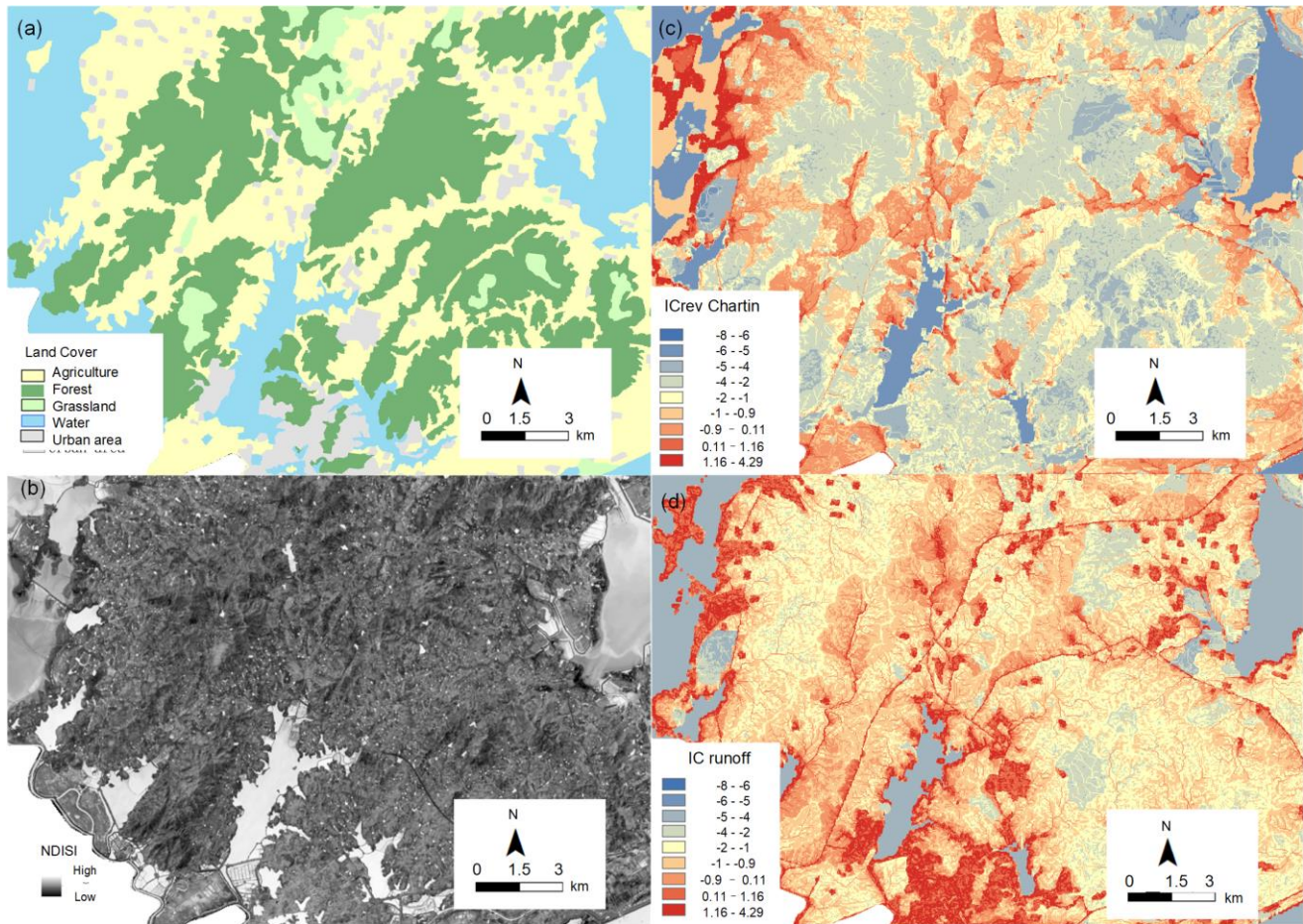


**Figure 8.** Effect of land use and NDISI on the index of runoff connectivity (IC). Map details of Lake Liancheng near the Yangtze River: (a) Land cover, (b) NDISI, (c)  $IC_{rev\ Chartin}$ , (d)  $IC_{runoff}$ .

variation. In contrast, the DEM data within the lake show limited slope variation, and therefore low connectivity (Figure 6a). The same situation was observed in Lake Caizi and Lake Fengsha. If DEM data or lake bottom terrain data with high resolution were available, it would be possible to obtain more accurate connectivity results for Lake Baidang (Liu et al., 2020).

The analysis results show that in April and July, the  $IC_{runoff}$  and  $IC_{thermal}$  of the Huanghu and Shun'an rivers had a consistent trend. In December, the  $IC_{runoff}$  of the Huanghu River was greater than that of the Shun'an River (Table 2), while the  $IC_{thermal}$  of the Shun'an River was greater than that of the Huanghu River (Table 3). This shows that differences in hydrological connectivity depend on the evaluation different parameters (Liu, 2020). The same results were observed at the sampling sites (Figure 7): both the  $IC_{runoff}$  and the  $IC_{thermal}$  in July were greater than those in August. It is noteworthy that the river temperature in August was higher than that in July, but, as mentioned above, the effect of upstream water on water temperature (Caissie, 2006) was not considered in the present study.

Rainfall erosivity is an important parameter, highly applicable to natural watersheds with permeable surfaces. In the present study, the  $IC_{rev\ Chartin}$  (Figure 8), an index based on rain-

fall erosivity (Chartin et al., 2017; Liu et al., 2020), was applied to the study area. It is noteworthy that using different weighting factors determines significant variations in the runoff connectivity values obtained. For example, when  $IC_{thermal}$  is used, the connectivity of urban areas is moderate, but when  $IC_{runoff}$  is used, it is high. These varying data cannot be detected from the  $IC_{thermal}$ , because rainfall erosivity does not reveal the attribute characteristics of the underlying surface, and the increase of impervious surface attributes can reflect runoff collection more comprehensively (Figure 8). Therefore, due to the different properties of the underlying surface, similar rainfall inputs in similar predetermined conditions do not always produce the same outputs (Bracken et al., 2007; Ali et al., 2012).

### 4.3. Implications for the Protection of Urban River-Lake Systems

At present, governmental agencies consider more about the impact of industrial wastewater on river-lake system, ignoring the impact of urbanization (Li et al., 2013). Therefore, the understanding of the spatial mechanisms of runoff and thermal connectivity has become an urgent priority for the protection of urban areas and its river-lake system (Coutant, 1999;

Poole and Berman, 2001). In this study, high connectivity was shown to be concentrated around the river-lake system and in downtown areas, therefore, the impact of regional runoff and thermal energy on river-lake systems and on the organisms living within them, should be fully considered in urban planning and management. Different protection strategies should be adopted in different areas. For example, when considering Lake Liancheng near the Yangtze River (Figure 8; Appendix: Figure S5), the connectivity of the south side of the lake is high due to the presence of impervious surfaces caused by urbanization, leading to a higher risk of levee collapse during the flood season; as a result, specific restoration methods are needed in this particular area. Instead of increasing hydrological connectivity (Meng et al., 2020), here the restoration strategy should not only consider the optimization of land use and the limitation of surface runoff connectivity (Dong et al., 2019), but also an increase in the number of paths for water resource allocation, to relieve flood pressure. In addition, ecohydrology and the sensitivity of thermal energy to human disturbance are important variables that resource managers should carefully consider (Coutant, 1999; Poole and Berman, 2001). To comprehensively protect the ecology of aquatic ecosystems in urban watersheds, thermal pollution associated with urban runoff should be taken into account. The present study provides a basic reference for future investigations of thermal variation occurring in river-lake systems within urban environments (Turko et al., 2020).

## 5. Conclusions

We defined the runoff and thermal connectivity of river-lake systems in urban areas and proposed a conceptual and mathematical framework to evaluate connectivity based on available data. This proposed method takes into account several factors affecting the generation, transportation and thermal conversion of both runoff and thermal energy, including land use, impervious coefficient, vegetation cover, terrain gradient, air temperature, and surface temperature. The mathematical framework can reveal the main sources of runoff and thermal energy in river-lake system. The model can be applied to different spatial scales, and its resolution and accuracy depend on the resolution and accuracy of the input data (Liu, et al., 2020). The new method was applied to a typical Chinese city where urbanization is currently increasing, posing significant risks to its river-lake system. The proposed approach proved successful in describing runoff and thermal connectivity, and it specifically identified differences in the spatio-temporal patterns between the two variables within an urbanized area. In addition, this method allowed for an improved estimation of hydrological connectivity parameters under different climatic conditions. Overall, the results of this study provide an important reference for future research on the optimization of runoff and thermal connectivity of river-lake systems in urban area.

**Declaration of competing interest.** The authors declare that they have no conflict of interest.

**Acknowledgments.** We thank the Tongling Ecological Environment

Bureau for supporting our research. This work was supported by the Key Project of the National Science Foundation of China (No. U1901212 and No. U2243208), the National Postdoctoral Program for Innovative Talents (No. BX20220040), and the General Program of China Postdoctoral Science Foundation (2022M710413).

## References

- Ali, G., Oswald, C., Spence, C. and Wellen, C. (2018). The T-TEL method for assessing water, sediment, and chemical connectivity. *Water Resour. Res.*, 54(2), 634-662. <http://doi.org/10.1002/2017WR020707>
- Ali, G., Tetzlaff, D., Soulsby, C. and McDonnell, J.J. (2012). Topographic, pedologic and climatic interactions influencing streamflow generation at multiple catchment scales. *Hydrol. Process.*, 26(25), 3858-3874. <http://doi.org/10.1002/hyp.8416>
- Biemans, H., Haddeland, I., Kabat, P., Ludwig, F., Hutjes, R.W.A., Heinke, J. and Gerten, D. (2011). Impact of reservoirs on river discharge and irrigation water supply during the 20th century. *Water Resour. Res.*, 47(3), 77-79. <https://doi.org/10.1029/2009WR008929>
- Binti Md, A., Yassin, A., Bond, S. and McDonagh, J. (2011). Developing guidelines for riverfront developments for Malaysia. *PRPRJ*, 17(4), 511-530. <http://doi.org/10.1080/14445921.2011.11104340>
- Bracken, L.J. and Croke, J. (2007). The concept of hydrological connectivity and its contribution to understanding runoff-dominated geomorphic systems. *Hydrol. Process.*, 21(13), 1749-1763. <http://doi.org/10.1002/hyp.6313>
- Bracken, L.J., Wainwright, J., Ali, G., Roy, A.G., Smith, M.W. and Tetzlaff, D. (2013). Concepts of hydrological connectivity: Research approaches, pathways and future agendas. *Earth Sci. Rev.*, 119, 17-34. <https://doi.org/10.1016/j.earscirev.2013.02.001>
- Bracken, L.J., Turnbull, L., Wainwright, J. and Bogaart, P. (2015). Sediment connectivity: A framework for understanding sediment transfer at multiple scales. *Earth Surf. Process. Landf.*, 40(2), 177-188. <https://doi.org/10.1002/esp.3635>
- Borah, D.K., Yagow, G., Saleh, A., Barnes, P.L., Rosenthal, W., Krug, E.C. and Hauck, L.M. (2006). Sediment and nutrient modeling for TMDL development and implementation. *Trans. ASABE*, 49(4), 967-986. <https://doi.org/10.13031/2013.21742>
- Borselli, L., Cassi, P. and Torri, D. (2008). Prolegomena to sediment and flow connectivity in the landscape: A GIS and field numerical assessment. *Catena (Amst)*, 75(3), 268-277. <https://doi.org/10.1016/j.catena.2008.07.006>
- Booth, D.B., Kraseski, K.A. and Jackson, C.R. (2014). Local-scale and watershed-scale determinants of summertime urban stream temperatures. *Hydrol. Process.*, 28(4), 2427-2438. <https://doi.org/10.1002-hyp.9810>
- Caissie, D. (2006). The thermal regime of rivers: A review. *Freshw. Biol.*, 51, 1389-1406. <https://doi.org/10.1111/j.1365-2427.2006.01597.x>
- Cavalli, M., Trevisani, S., Comiti, F. and Marchi, L. (2013). Geomorphometric assessment of spatial sediment connectivity in small Alpine catchments. *Geomorphology (Amst)*, 188(15), 31-41. <https://doi.org/10.1016/j.geomorph.2012.05.007>
- Chappell, J., McKay, S.K., Freeman, M.C. and Pringle, C.M. (2019). Long-term (37 years) impacts of low-head dams on freshwater shrimp habitat connectivity in northeastern Puerto Rico. *River Res. Appl.*, 35(7), 1034-1043. <https://doi.org/10.1002/rra.3499>
- Chartin, C., Evrard, O., Laceby, J.P., Onda, Y., Otlé, C., Lefèvre, I. and Cerdan, O. (2017). The impact of typhoons on sediment connectivity: lessons learnt from contaminated coastal catchments of the Fukushima Prefecture (Japan). *Earth Surf. Process. Landf.*, 42(2), 306-317. <https://doi.org/10.1002/esp.4056>
- Che, Y., Yang, K., Chen, T. and Xu, Q. (2012). Assessing a riverfront rehabilitation project using the comprehensive index of public accessibility. *Ecol. Eng.*, 40, 80-87. <https://doi.org/10.1016/j.eco>

- len-g.2011.12.008
- Chen, Y., Wang, Y.G. and Chen, K. (2020). Planning and management framework of river system connectivity in the construction of sponge city. *Urban Flood Control*, 30(7), 10-15. <https://doi.org/10.16867/j.issn.1673-9264.2019279>
- China Economic Times. (2013). *Aquaculture insurance: easy consensus but difficult implementation*. [https://lib.cet.com.cn/paper/szb\\_c on/169968.html](https://lib.cet.com.cn/paper/szb_c on/169968.html)
- Coutant, C.C. (1999). *Perspectives on temperature in the Pacific Northwest's fresh waters*. Oak Ridge National Lab., TN (US), pp 1-124. <https://doi.org/10.2172/9042>
- Covino, T. (2017). Hydrologic connectivity as a framework for understanding biogeochemical flux through watersheds and along fluvial networks. *Geomorphology (Amst)*, 277, 133-144. <https://doi.org/10.1016/j.geomorph.2016.09.030>
- Croghan, D., Van Loon, A.F., Sadler, J.P., Bradley, C. and Hannah, D.M. (2019). Prediction of river temperature surges is dependent on precipitation method. *Hydrol. Process.*, 33(1), 144-159. <https://doi.org/10.1002/hyp.13317>
- Crook, K.E., Pringle, C.M. and Freeman, M.C. (2009). A method to assess longitudinal riverine connectivity in tropical streams dominated by migratory biota. *Aquat. Conserv.*, 19(6), 714-723. <https://doi.org/10.1002/aqc.1025>
- Croke, J., Mockler, S., Fogarty, P. and Takken, I. (2005). Sediment concentration changes in runoff pathways from a forest road network and the resultant spatial pattern of catchment connectivity. *Geomorphology (Amst)*, 68(3-4), 257-268. <https://doi.org/10.1016/j.g-eooph.2004.11.020>
- Croke, J., Fryirs, K. and Thompson, C. (2013). Channel-floodplain connectivity during an extreme flood event: implications for sediment erosion, deposition, and delivery. *Earth Surf. Process. Landf.*, 38(12), 1444-1456. <https://doi.org/10.1002/esp.3430>
- Dong, R., Zhang, X. and Li, H. (2019). Constructing the ecological security pattern for sponge city: a case study in Zhengzhou, China. *Water*, 11(2), 284. <https://doi.org/10.3390/w11020284>
- Endreny, T.A., Somerlot, C. and Hassett, J.M. (2003). Hydrograph sensitivity to estimates of map impervious cover: a WinHSPF BASINS case study. *Hydrol. Process.*, 17(5), 1019-1034. <https://doi.org/10.1002/hyp.1178>
- Feng, X.M., Zhang, Y.F., Xu, G.Y., He, C.D. and Huang C.Y. (2020). Rainwater temperature prediction and typical urban surface energy characteristics during rainfall in the hot-humid region. *Build. Sci.*, 36(10), 176-184. <https://doi.org/10.13614/j.cnki.11-1962/tu.2020.10.24>
- Fletcher, T.D., Andrieu, H. and Hamel, P. (2013). Understanding, management and modelling of urban hydrology and its consequences for receiving waters: A state of the art. *Adv. Water Resour.*, 51, 261-279. <https://doi.org/10.1016/j.advwatres.2012.09.001>
- Freeman, M.C., Pringle, C.M. and Jackson, C.R. (2007). Hydrologic connectivity and the contribution of stream headwaters to ecological integrity at regional scales. *J. Am. Water Resour. Assoc.*, 43(1), 5-14. <https://doi.org/10.1111/j.1752-1688.2007.00002.x>
- Gomi, T., Sidle, R.C., Miyata, S., Kosugi, K. and Onda, Y. (2008). Dynamic runoff connectivity of overland flow on steep forested hillslopes: scale effects and runoff transfer. *Water Resour. Res.*, 44(8), 2493-2503. <https://doi.org/10.1029/2007WR005894>
- Grill, G., Lehner, B., Thieme, M. Geenen, B., Tickner, D., Antonelli, F., Babu, S., Borrelli, P., Cheng, L., Crochetiere, H., Ehalt Macedo, H., Filgueiras, R., Goichot, M., Higgins, J., Hogan, Z., Lip, B., McClain, M.E., Meng, J., Mulligan, M., Nilsson, C., Olden, J.D., Opperman, J.J., Petry, P., Reidy Liermann, C., Sáenz, L., Salinas-Rodríguez, S., Schelle, P., Schmitt, R.J.P., Snider, J., Tan, F., Tockner, K., Valdujo, P.H., van Soesbergen, A. and Zarfl, C. (2019). Mapping the world's free-flowing rivers. *Nature*, 569(7755), 215-221. <https://doi.org/10.1038/s41586-019-1111-9>
- Haq, R.U. and James, W. (2002). Thermal enrichment of stream temperature by urban storm waters. In *Global Solutions for Urban Drainage, Proc. of the Ninth International Conference on Urban Drainage (9ICUD)*, pp. 1-11. [https://doi.org/10.1061/40644\(2002\)-195](https://doi.org/10.1061/40644(2002)-195)
- Hassett, B.A., Sudduth, E.B., Somers, K.A., Urban, D.L., Violin, C.R., Wang, S.Y., Wright, J.P., Cory, R.M. and Bernhardt, E.S. (2018). Pulling apart the urbanization axis: patterns of physiochemical degradation and biological response across stream ecosystems. *Freshw. Sci.*, 37(3), 653-672. <https://doi.org/10.1086/699387>
- Herb, W.R., Janke, B., Mohseni, O. and Stefan, H.G. (2008). Thermal pollution of streams by runoff from paved surfaces. *Hydrol. Process.*, 22(7), 987-999. <https://doi.org/10.1002/hyp.6986>
- Horne, J.P. and Hubbart, J.A. (2020). A spatially distributed investigation of stream water temperature in a contemporary mixed-land-use watershed. *Water*, 12(1756), 1-25. <https://doi.org/10.3390/w12061756>
- Janke, B.D., Herb, W.R., Mohseni, O. and Stefan, H.G. (2009). Simulation of heat export by rainfall-runoff from a paved surface. *J. Hydrol.*, 365(3-4), 195-212. <http://doi.org/10.1016/j.jhydrol.2008.11.019>
- Jencso, K.G., McGlynn, B.L., Gooseff, M.N., Wondzell, S.M., Ben-cala, K.E., and Marshall, L.A. (2009). Hydrologic connectivity between landscapes and streams: transferring reach and plot-scale understanding to the catchment scale. *Water Resour. Res.*, 45, W044428. <https://doi.org/10.1029/2008WR007225>
- Jia, Y.G., Ni, G.H., Kawahara, Y. and Suetsugi, T. (2001). Development of WEP model and its application to an urban watershed. *Hydrol. Process.*, 15, 2175-2194. <https://doi.org/10.1002/hyp.275>
- Kalantari, Z., Cavalli, M., Cantone, C. Crema, S. and Destouni, G. (2017). Flood probability quantification for road infrastructure: Data-driven spatial-statistical approach and case study applications. *Sci. Total Environ.*, 581-582, 386-398. <https://doi.org/10.1016/j.scitotenv.2016.12.147>
- Kinouchi, T.; Yagi, H. and Miyamoto, M. (2007). Increase in stream temperature related to anthropogenic heat input from urban wastewater. *J. Hydrol.*, 335(1-2), 78-88. <https://doi.org/10.1016/j.jhydrol.2006.11.002>
- Liang, C., Zhang, X., Xia, J., Xu, J. and She, D. (2020). The effect of sponge city construction for reducing directly connected impervious areas on hydrological responses at the urban catchment scale. *Water*, 12(4), 1163. <https://doi.org/10.3390/w12041163>
- Li, X.J., Li, J.Q., Qi, H.J., Sun, K. and Song, R. (2013). Advance in thermal pollution of urban rainfall runoff and its mitigation measures. *Adv. Water Resour.*, 33(1), 89-94. <https://doi.org/10.388-0/j.issn.1006-7647.2013.01.020>
- Li, Z.L., Zhou, X.B., Zhao, X.H., Mei, P.W., Zhang, Z. and Wang, Y.Q. (2017). Estimating pollution load and evaluating management practices for Yuqiao Reservoir watershed. *Environ. Pollut. and Control.*, 39(7), 752-756. <https://doi.org/10.15985/j.cnki.1001-386-5.2017.07.012>
- Liu, Y.L., Cui, B.S., Du, J.Z., Wang, Q., Yu, S.L. and Yang, W. (2020). A method for evaluating the longitudinal functional connectivity of a river-lake-marsh system and its application in China. *Hydrol. Process.*, 34, 5278-5297. <https://doi.org/10.1002/hyp.13946>
- López-Vicente, M., Pérez-Bielsa, C., López-Montero, T., Lambán, L.J. and Navas, A. (2014). Runoff simulation with eight different flow accumulation algorithms: recommendations using a spatially distributed and open-source model. *Environ. Model. Softw.*, 62, 11-21. <https://doi.org/10.1016/j.envsoft.2014.08.025>
- Lu, G.Y. and Wong, D.W. (2008). An adaptive inverse-distance weighting spatial interpolation technique. *Comput. Geosci.*, 34(9), 1044-1055. <https://doi.org/10.1016/j.cageo.2007.07.010>
- Martin, C.J., Hodges, C. and Dymond, R. (2019). Geospatial method to map potential risk of stormwater thermal pollution. *J. Am. Water Resour. Assoc.*, 55(2), 511-522. <https://doi.org/10.1111/1752-168-8.12732>

- Meng, B., Liu, J.L., Bao, K. and Sun, B. (2020). Methodologies and management framework for restoration of wetland hydrologic connectivity: A Synthesis. *Integr. Environ. Assess. Manag.*, 16(4), 438-451. <https://doi.org/10.1002/ieam.4256>
- Nelson, K.C. and Palmer, M.A. (2007). Stream temperature surges under urbanization and climate change: Data, models, and responses. *J. Am. Water Resour. Assoc.*, 43(2), 440-452. <https://doi.org/10.1111/j.1752-1688.2007.00034.x>
- Oldham, C.E., Farrow, D.E. and Peiffer, S. (2013). A generalized dam-köhler number for classifying material processing in hydrological systems. *Hydrol. Earth Syst. Sci.*, 17(3), 1133-1148. <https://doi.org/10.5194/hess-17-1133-2013>
- O'Driscoll, M.A. and DeWalle, D.R. (2006). Stream-air temperature relations to classify stream-ground water interactions in a karst setting, central Pennsylvania, USA. *J. Hydrol.*, 329(1-2), 140-153. <https://doi.org/10.1016/j.jhydrol.2006.02.010>
- Paul, M.J. and Meyer, J.L. (2001). *Streams in the urban landscape*. Springer, Boston, MA, pp 207-231. [https://doi.org/10.1007/978-0-387-73412-5\\_12](https://doi.org/10.1007/978-0-387-73412-5_12)
- Petty, J.T., Hansbarger, J.L., Huntsman, B.M. and Mazik, P.M. (2012). Brook trout movement in response to temperature, flow, and thermal refugia within a complex Appalachian riverscape. *Trans. Am. Fish. Soc.*, 141(4), 1060-1073. <https://doi.org/10.1080/000284-87.2012.681102>
- Pollock, M.M., Beechie, T.J., Liermann, M. and Bigley, R.E. (2009). Stream temperature relationships to forest harvest in western Washington. *J. Am. Water Resour. Assoc.*, 45(1), 141-156. <https://doi.org/10.1111/j.1752-1688.2008.00266.x>
- Poole, G.C. and Berman, C.H. (2001). An ecological perspective on in-stream temperature: Natural heat dynamics and mechanisms of human-caused thermal degradation. *Environ. Manage.*, 27(6), 787-802. <https://doi.org/10.1007/s002670010188>
- Pringle, C.M. (2001). Hydrologic connectivity and the management of biological reserves: A global perspective. *Ecol. Appl.*, 11(4), 981-998. [https://doi.org/10.1890/1051-0761\(2001\)011\[0981:HCATM-O\]2.0.CO;2](https://doi.org/10.1890/1051-0761(2001)011[0981:HCATM-O]2.0.CO;2)
- Pringle, C. (2003). What is hydrologic connectivity and why is it ecologically important? *Hydrol. Process.*, 17, 2685-2689. <https://doi.org/10.1002/hyp.5145>
- Regier, P.J., González-Pinzón, R., Van Horn, D.J., Reale, J.K., Nichols, J. and Khandewal, A. (2020). Water quality impacts of urban and non-urban arid-land runoff on the Rio Grande. *Sci. Total Environ.*, 729, 138443. <https://doi.org/10.1016/j.scitotenv.2020.138443>
- Renard, K.G., Foster, G.R., Weessies, G.A., Mc Cool, D.K. and Yodler, D.C. (1997). *Predicting soil erosion bywater - a guide to conservation planning with the Revised Universal Soil Loss Equation (RUSLE)*. U.S.D.A.-A.R.S., Washington State University, Pullman, WA. pp. 1-408. ISBN: 0160489385
- Roa-Espinosa, A., Wilson, T.B., Norman, J.M. and Johnson, K. (2003). Predicting the impact of urban development on stream temperature using a thermal urban runoff model (TURM). *National Conference on Urban Stormwater: Enhancing Programs at the Local Level*, Chicago, pp 369-389.
- Sabouri, F., Gharabaghi, B., Mahboubi, A.A. and McBean, E.A. (2013). Impervious surfaces and sewer pipe effects on stormwater runoff temperature. *J. Hydrol.*, 502(1), 10-17. <https://doi.org/10.1016/j.jhydrol.2013.08.016>
- Soil Conservation Service (SCS). (1972). National Engineering Handbook, Section 4: *Hydrology*. Department of Agriculture, Washington, D.C., 762 p.
- Sinokrot, B.A. and Stefan, H.G. (1993). Stream temperature dynamics: Measurements and modeling. *Water Resour. Res.*, 29(7), 2299-2312. <https://doi.org/10.1029/93WR00540>
- Smith, M.W., Bracken, L.J. and Cox, N.J. (2010). Toward a dynamic representation of hydrological connectivity at the hillslope scale in semiarid areas. *Water Resour. Res.*, 46(12), 65-74. <https://doi.org/10.1029/2009WR008496>
- Tang, H.B. (2016). Estimation of the return period of the 2016 flood in the Chenyao Lake Basin, Anhui Province. *Zhihuai*. (12), 57. <https://kns.cnki.net/kcms/detail/detail.aspx?dbcode=CJFD&dbname=CJFDLAST2017&filename=ZIHU201612037&v=SyHQIdcljDrxGU70KvnQ41nzc5Iortybsl7x4xn29IyBS1%25mmd2BiTFlowldqC9AaGhMj> (in Chinese)
- Thompson, A.M., Wilson, T., Norman, J.M., Gemechu, A.L and Roa-Espinosa, A. (2008). Modeling the effect of summertime heating on urban runoff temperature. *J. Am. Water Resour. Assoc.*, 44(6), 1548-1563. <https://doi.org/10.1111/j.1752-1688.2008.00259.x>
- Turko, A.J., Nolan, C.B., Balshine, S., Scott, G.R. and Pitcher, T.E. (2020). Thermal tolerance depends on season, age and body condition in imperilled redbreasted dace *Clinostomus elongatus*. *Conserv. Physiol.*, 8(1), coaa062. <https://doi.org/10.1093/conhy/c-0aa062>
- Turnbull, L., Wainwright, J. and Brazier, R.E. (2008). A conceptual framework for understanding semi-arid land degradation: Ecological interactions across multiple space and time scales. *Ecohydrology*, 1(1), 23-34. <https://doi.org/10.1002/eco.4>
- USEPA (2001). *PLOAD version 3.0: An ArcView GIS Tool to calculate nonpoint sources of pollution in watersheds and stormwater projects*. EPA WDC0101-HSQ. Washington: U.S. Environmental Protection Agency.
- Van Buren, M.A., Watt, W.E., Marsalek, J. and Anderson, B.C. (2000). Thermal enhancement of stormwater runoff by paved surfaces. *Water Res.*, 34(4), 1359-1371. [https://doi.org/10.1016/S0043-1354\(9-9\)00244-4](https://doi.org/10.1016/S0043-1354(9-9)00244-4)
- Walsh, C.J., Roy, A.H., Feminella, J.W., Cottingham, P.D., Groffman, P.M. and Morgan, R.P. (2005). The urban stream syndrome: Current knowledge and the search for a cure. *J. North Am. Benthol. Soc.*, 24(3), 706-723. <https://doi.org/10.1899/04-028.1>
- Walsh, C.J., Fletcher, T.D. and Burns, M.J. (2012). Urban stormwater runoff: A new class of environmental flow problem. *PLoS One*, 7(9), e45814. <https://doi.org/10.1371/journal.pone.0045814>
- Wainwright, J., Turnbull, L., Ibrahim, T.G., Lexartza-Artza, I., Thornton, S.F. and Brazier, R.E. (2011). Linking environmental regimes, space, and time: Interpretations of structural and functional connectivity. *Geomorphology (Amst)*, 126(3), 387-404. <https://doi.org/10.1016/j.geomorph.2010.07.027>
- Wang, B.Z., Bi, R.T., Chen, L.G. and Jing, Y.D. (2020). Soil erosion in loss area of the upstream of the Hutuo River: Spatial characteristics based on USLE model. *Chin. Agric. Sci. Bull.*, 36(7), 76-82. <https://doi.org/casb20190900654>
- Wang, W. (2018). Study on design flood calculation method of Baidang Lake. *J. Anhui Agric. Sci.*, 18(2), 17-20. [https://doi.org/1671-6221\(2018\)02-0017-04](https://doi.org/1671-6221(2018)02-0017-04)
- Webb, B.W. and Nobilis, F. (1997). Long-term perspective on the nature of the water-air temperature relationship-A case study. *Hydrol. Process.*, 11(2), 137-147. [https://doi.org/10.1002/\(SICI\)1099-1085\(199702\)11:2<137::AID-HYP405>3.0.CO;2-2](https://doi.org/10.1002/(SICI)1099-1085(199702)11:2<137::AID-HYP405>3.0.CO;2-2)
- Webb, B.W., Hannah, D.M., Moore, R.D., Brown, L.E. and Nobilis, F. (2008). Recent advances in stream and river temperature research. *Hydrol. Process.*, 22(7), 902-918. <https://doi.org/10.1002/hyp.6994>
- Webster, J.R. (2007). Spiraling down the river continuum: Stream ecology and the U-shaped curve. *J. North Am. Benthol. Soc.*, 26(3), 375-389. <https://doi.org/10.1899/06-095.1>
- Wegener, P., Covino, T. and Wohl, E. (2017). Beaver-mediated lateral hydrologic connectivity, fluvial carbon and nutrient flux, and aquatic ecosystem metabolism. *Water Resour. Res.*, 53(6), 4606-4623. <https://doi.org/10.1002/2016WR019790>
- Wohl, E., Rathburn, S., Chignell, S., Garrett, K., Laurel, D., Livers, B., Patton, A., Records, R., Richards, M., Schook, D.M., Sutfin, N.A. and Wegener, P. (2017). Mapping longitudinal stream connectivity in the North St. Vrain Creek watershed of Colorado. *Geomorphology (Amst)*, 277, 171-181. <https://doi.org/10.1016/j.ge-morph.2016.05.004>

- Xu, H.Q. (2008). A new remote sensing index for fastly extracting impervious surface. *Geo. Infor. Sci. Wuhan Univ.*, 33(11), 1150-1153. [https://doi.org/1671-8860\(2008\)11-1150-04](https://doi.org/1671-8860(2008)11-1150-04)
- Xu, W.T., Wang, J.L., Wu, Y.J. and Lv, Y.J. (2020). Advances in research on thermal pollution characteristics, load assessment and control measures of urban stormwater runoff. *Environ. Engin.* 38(4), 26-58. <https://doi.org/10.13205/j.hjgc.202004006> (in Chinese)
- Zhang, Z.Z., Xiong, K.N. and Huang, D.H. (2018). Analysis of temporal and spatial changes and influencing factors of vegetation coverage on Fanjing Mountain in the past 30 years. *Res. Soil Water Conserv.*, 25(2), 183-189. <https://doi.org/10.13869/j.cnki.rswc.2018.02.026> (in Chinese)